Continuous Flow Mesofluidic Synthesis of Cu_2ZnSnS_4 Nanoparticle Inks

Brendan Flynn, [a] Ian Braly, [a] Philip A. Glover, [a] Richard P. Oleksak, [a] Chris Durgan, [a] and Gregory S. Herman [a*]

[a]Oregon State University, School of Chemical, Biological and Environmental Engineering, 102 Gleeson Hall, Corvallis, OR USA 97331-2702

*Corresponding author. Email: greg.herman@oregonstate.edu. Phone: 1-541-737-2496. Fax: 1-541-737-4600.

Abstract

Copper zinc tin sulfide (CZTS) nanoparticles were synthesized using ethylene glycol as a solvent via a continuous flow mesofluidic reactor. In this study reaction temperature, residence time, and precursor concentrations were used to control CZTS composition. It was found that CZTS initially forms by the nucleation of $Cu_{2-x}S$ with subsequent incorporation of the remaining metal species as dictated by the cation reactivity, where $Cu^{+} > Sn^{+4} > Zn^{+2}$. CZTS nanoparticle films annealed in a selenium-containing atmosphere resulted in the formation of copper zinc tin selenide nanoparticles with much larger particle sizes.

Keywords: Copper zinc tin sulfide; Copper zinc tin selenide; Solar energy materials; Nanocrystalline materials; Nanoparticles; Colloidal processing

1. Introduction

Copper zinc tin sulfide (CZTS) is a good absorber candidate for low cost thin film solar cells due to its excellent optical properties[1, 2] and relatively high abundance of its constituent elements. CZTS is isoelectronic with copper indium gallium diselenide (CIGS), which is currently used in commercial thin film solar modules[3]. In 2012, the prices of indium and gallium were roughly 275 times that of zinc and 15 times that of tin[4]. For high volume solar cell production, CZTS would likely provide significant cost advantages compared to CIGS due to the relatively lower cost of zinc and tin, provided comparable solar cell efficiencies are obtained[5]. Solution processing of CZTS offers a low cost and high throughput alternative to vacuum based methods[6]. Several different solution based approaches to synthesizing CZTS have been studied, where the focus has been on batch synthetic methods[7-10]. Hydrazine[11, 12], electroplating[13], sol-gel [14, 15], spray pyrolysis[16], solvothermal[17], and microwave-assisted[18] methods have also been used to synthesize CZTS for solar cells. Recently it has been demonstrated that continuous flow processes have potential for the large scale, solution based synthesis of CZTS nanomaterials[19]. Further studies on reaction chemistries and conditions are required to optimize CZTS continuous flow synthetic approaches.

In this study we investigated the synthesis of CZTS nanoparticles utilizing a mesofluidic continuous flow reactor with triethylene glycol, a low-cost solvent. The flow in the reactor was segmented in a controlled manner by gas generation within the reaction stream to assist in narrowing the nanoparticle size distribution and minimize

clogging. It was found that the nanoparticle composition could be controlled by optimizing the residence time, reaction temperature, and concentration of precursors.

2. Experimental methods

Triethylene glycol (TEG) was used to dissolve cuprous chloride (0.005 M), zinc chloride (0.00545 M), and stannic chloride pentahydrate (0.00286M) and in a separate beaker thioacetamide (C_2H_5NS, 0.0226 M). Room temperature precursor solutions were pumped through separate preheating coils using a peristaltic pump. The reactor used perfluoroalkoxy (PFA) tubing (ID = 1.59 mm). Burst nucleation of the nanoparticles occurred in a mesofluidic T-mixer (Parker GTC-2) with a minimum diameter of 2.38 mm. The liquid flow was self-segmented by gas produced within the reactor by evaporation of the solvent, release of dissolved gas, and/or decomposition of thioacetamide to hydrogen sulfide. After nucleation, the solution flowed through PFA tubing submerged in a heated bath. At the exit of the bath, polyether ether ketone (PEEK) tubing (ID = 0.76 mm) was attached and placed in an ice bath. The nanoparticle reaction products were washed several times in deionized water and ethanol prior to analysis. Annealing studies were performed at 500 °C for 20 minutes in a tube furnace under flowing nitrogen (300 mL/min at 15 kPa system pressure), without or with sulfur or selenium powders. These conditions are referenced as N_2, N_2+S, and N_2+Se, respectively.

Nanoparticle film morphology and composition was determined using a FEI Quanta 3D (30 kV beam energy) by scanning electron microscopy and energy dispersive X-ray spectroscopy (EDS), respectively. Raman spectra were obtained with a Horiba-Jobin Yvon HR800 Raman spectrometer with 532 nm radiation. X-ray

diffraction (XRD) analysis was performed with a Bruker D8 Discover diffractometer with Cu Kα radiation. The composition of the precursor solution and post-reaction supernatant were analyzed by inductively coupled plasma atomic emission spectroscopy (ICP-AES) using a Varian Liberty 150 spectrometer. High resolution imaging of the as synthesized particles was performed using a FEI Titan FEG transmission electron microscope (TEM).

3. Results and Discussion

Residence time had a pronounced effect on the composition and size of the CZTS nanoparticles. Initial studies were performed with stoichiometric precursor solutions reacted at 215 °C for residence times $\tau < 1$, $\tau = 28$, and $\tau = 49$ minutes. EDS results are given in Table 1. As residence time increased, the relative copper content decreased while sulfur content increased. Significant zinc content was only observed for $\tau > 28$ min. The XRD spectra in Fig. 1 (a) show four main diffraction peaks at 2θ = 28.4°, 32.9°, 47.3°, and 56.0°, which correspond to the (112), (200)/(004), (220)/(204), and (312)/(116) planes of kesterite CZTS. These planes were indexed using JCPDS 26-0575 and by simulating the CZTS structure with JEMS software[20] and are shown as the reference pattern at the top of Fig. 1 (a). Performing a Scherrer analysis on the (112) peak for CZTS nanoparticles reacted for $\tau < 1$, $\tau = 28$, and $\tau = 49$ min gave particle sizes of 7.6 nm, 8.6 nm, and 13.8 nm, respectively. The Raman spectra in Fig. 1 (b) have two main peaks at ~289 and 332 cm^{-1}. These peaks have previously been assigned to the A_1 vibrational modes in the CZTS lattice [21]. A large increase in the relative intensity of the peak positioned at 332 cm^{-1} was found for $\tau = 49$ min, which may be related to the incorporation of zinc, the larger size of the nanoparticles, and/or

greater crystalline order of the nanoparticles. In a prior study, a comparison of Raman spectra from CZTS and tetragonal Cu_2SnS_3 thin films reveal an analogous intensity increase for the 332 cm^{-1} peak for CZTS[22]. In addition, the tetragonal Cu_2SnS_3 Raman spectrum is nearly identical in shape and relative peak intensity compared to the Raman spectra obtained for τ < 1min and τ = 28 min reactions in this study, suggesting the formation of Cu_2SnS_3 at shorter residence times. The position of the Raman peak at 331-332 cm^{-1} has been reported for both CZTS thin films[23] and nanoparticles[24], but was red shifted compared to typical values of ~336-339 cm^{-1}[21, 22]. The small nanoparticle size combined with cation disorder may contribute to the broad red shifted 332 cm^{-1} peak observed in this study[25, 26]. The relative metal cation reaction rates were estimated by comparing the composition of the metal precursor solutions with stoichiometric metal cation concentrations and the post-reaction supernatant using ICP-AES. Only 0.23% of the initial copper, 9% of the initial tin, and 20% of the initial zinc remained in the post-reaction supernatant for τ < 1 min. Relative reaction rates for the metal cations were estimated to be $Cu^{+}>Sn^{4+}>Zn^{2+}$, which is consistent with our EDS analysis of the CZTS nanoparticles shown in Table 1. This is also in agreement with a prior continuous flow CZTS nanoparticle study where increasing residence time resulted in a decrease in the copper content and an increase in the zinc content[19].

To obtain the desired CZTS nanoparticle stoichiometry we have optimized the reaction temperature, residence time, and initial concentration of precursors. Optimal reaction conditions were obtained at 230 °C with τ = 75 min and metal precursor solution composition ratios of Cu/(Zn+Sn) = 0.60 and Zn/Sn = 1.9. The sulfur precursor was in excess by 1.65x, based on the desired stoichiometry of Cu_2ZnSnS_4 and the

appropriate oxidation states of the ions in solution (i.e., Cu^{+}, Zn^{2+} and Sn^{4+}). For these reaction conditions no copper remained in the post-reaction supernatant, compared to 4% of the tin and 24% of the zinc, resulting in CZTS nanoparticles with the following composition $Cu_{1.9}Zn_{1.0}Sn_{1.2}S_{3.9}$. Both single and multicrystalline CZTS nanoparticles were synthesized as shown by the high-resolution TEM results in Fig. 2 (a) and (b). Fast Fourier transforms (FFT) of the TEM images are shown in Fig. 2 (c) and (d), and both types of nanoparticles can be indexed to the CZTS kesterite structure, where the diffraction spots correspond to the (220)/(204) and (332)/(316) planes as viewed along the [112] zone axis. The bright field TEM image in Fig. 2(e) shows individual CZTS nanoparticles, which have an average size of 5.4 nm with a standard deviation of 2.0 nm, as determined by measuring 50 nanoparticles. In Fig. 3 the lowermost XRD spectrum is for the as synthesized CZTS nanoparticles and has four broad diffraction peaks similar to the XRD patterns shown in Fig. 1 (a). The nanoparticle crystallite size was estimated to be 13.6 nm using the Scherrer analysis of the (112) diffraction peak. Agglomeration may prevent the observation of a representative distribution of nanoparticles, which may explain the discrepancy between particle sizing using TEM and XRD analysis.[27]. The Raman spectrum is shown in Fig. 3 (b) for the as synthesized CZTS nanoparticles where the A_1 vibrational modes of CZTS at 333 cm^{-1} and 288 cm^{-1} were observed, in close agreement with Raman data from other CZTS nanoparticle work[19]. For these reaction conditions there was no $Cu_{2-x}S$ formed as indicated by the absence of a Raman peak at 475 cm^{-1}.

The optimized CZTS nanoparticles were annealed at 500 °C for 20 min in nitrogen (N_2), sulfur (N_2+S), and selenium (N_2+Se). As shown in Fig. 3 (a) the XRD

peaks become narrower and more intense after each annealing treatment. CZTS crystallite sizes were calculated using the Scherrer method after annealing in N_2, N_2+S and N_2+Se ambient and were determined to be 25.3, 27.6, and 43.4 nm, respectively. After the N_2+Se anneal the main peaks at 2θ = 28.4°, 47.3°, and 56.0° all shift to smaller angles due to lattice expansion, as can be seen more clearly by the inset in Fig. 3. This N_2+Se annealing process leads to the formation of CZTSe from the CZTS starting material based on the magnitude of the peak shifts, and the absence of the peak at 2θ = 32.9°, which were consistent with the CZTSe reference pattern (JCPDS 52-0868) shown in the upper portion of the figure. The Raman spectra shown in Fig. 3 (b) confirms that sulfur was replaced by selenium in the nanoparticles after the N_2+Se anneal. For the as synthesized nanoparticles, and those annealed in N_2, and N_2+S, the main CZTS A_1 vibrational modes were observed. After the N_2+Se anneal these peaks were red-shifted, and the Raman spectrum was in good agreement with prior CZTSe studies[28, 29], with peaks located at 173 cm^{-1}, 193 cm^{-1}, and 232 cm^{-1}. This is consistent with the change in relative mass between S and Se, and that the A_1 vibrational modes in CZTS result from the motion of sulfur ions, and in CZTSe result from the motion of selenium ions.

4. Conclusion

Continuous flow methods show promise for the synthesis of CZTS. In this study CZTS nanoparticles were synthesized in a mesofluidic continuous flow reactor at modest temperatures using low cost solvents. Segmented flow was achieved within the reactor by the controlled generation of gas, which improved mixing of the nanoparticles and reduced particle size distributions. The CZTS nanoparticles were formed by a

multistep reaction where $Cu_{2-x}S$ initially formed, followed by the incorporation of Sn, and then finally Zn. Adjusting the initial precursor concentration, reaction time, and reaction temperature provided controlled of the CZTS stoichiometry. This approach allowed us to use metal precursors with equivalent counterions and avoid complex organic additives. Finally, the CZTS nanoparticles were converted to CZTSe after a N_2+Se anneal as indicated by EDS, XRD, and Raman data.

Acknowledgements

The authors would like to thank Hsiao-Wen Huang for assistance with the ICP-AES measurements. The authors gratefully acknowledge support from Sharp Laboratories of America and the National Science Foundation through CCI phase II grant number CHE-1102637 for the Center for Sustainable Materials Chemistry.

References:

[1] Seol J-S, Lee S-Y, Lee J-C, Nam H-D, Kim K-H. Sol Energ Mat Sol C 2003;75;155-62.
[2] Katagiri H. Thin Solid Films 2005;480; 426-32.
[3] Niki S, Contreras M, Repins I, Powalla M, Kushiya K, Ishizuka S, et al. Prog Photovoltaics Res Appl 2010;18;453-66.
[4] U.S. Geological Survey, Mineral commodity summaries 2013;1-201.
[5] Repins I, Vora N, Beall C, Wei SH, Yan Y, Romero M, et al. Mater Res Soc Symp P 2011;1324;97-108.
[6] Todorov T, Mitzi DB. Eur J Inorg Chem 2010;1;17-28.
[7] Shavel A, Arbiol J, Cabot A. J Am Chem Soc 2010;132;4514-5.
[8] Riha SC, Parkinson BA, Prieto AL. J Am Chem Soc 2011;133;15272-5.
[9] Guo Q, Hillhouse HW, Agrawal R. J Am Chem Soc 2009;131;11672-3.
[10] Jiang C, Lee JS, Talapin DV. J Am Chem Soc 2012;134;5010-3.
[11] Bag S, Gunawan O, Gokmen T, Zhu Y, Todorov TK, Mitzi DB, Energ Enivron Sci 2012;5;7060-5.
[12] Todorov TK, Tang J, Bag S, Gunawan O, Gokmen T, Zhu Y, et al. Adv Energy Mater 2013;3;34-8.
[13] Ahmed S, Reuter KB, Gunawan O, Guo L, Romankiw LT, Deligianni H. Adv Energy Mater 2012;2;253-9.
[14] Fischereder A, Rath T, Haas W, Amenitsch H, Albering J, Meischler D, et al. Chem Mater 2010;22;3399-406.
[15] Ki W, Hillhouse HW. Adv Energy Mater 2011;1;732-5.
[16] Kumar YBK, Babu GS, Bhaskar PU, Raja VS. Sol Energ Mat Sol C 2009;93;1230-7.
[17] Zhou Y-L, Zhou W-H, Li M, Du Y-F, Wu S-X. J Phys Chem C 2011;115;19632-9.
[18] Flynn B, Wang W, Chang C-h, Herman GS. Phys Status Solidi A 2012;209;2186-94.
[19] Shavel A, Cadavid D, Ibáñez M, Carrete A, Cabot A. J Am Chem Soc 2012;134;1438-41.
[20] Hall S, Szymanski J, Stewart J. Can Mineral 1978;16;131-7.
[21] Himmrich M, Haeuseler H. Spectrochim Acta A 1991;47;933-42.
[22] Fernandes PA, Salomé PMP, da Cunha AF. J Alloy Compd 2011;509;7600-6.
[23] Salome PMP, Malaquias J, Fernandes PA, Ferreira MS, da Cunha AF, Leitao JP, et al. Sol Energ Mater Sol C 2012;101;147-53.
[24] Zou C, Zhang L, Lin D, Yang Y, Li Q, Xu X, et al. CrystEngComm 2011;13;3310-3.
[25] Gouadec G, Colomban P. Prog Cryst Growth Ch 2007;53;1-56.
[26] Campbell IH, Fauchet PM. Solid State Commun 1986;58;739-41.
[27] Weibel A, Bouchet R, Boulc'h F, Knauth P. Chem Mater 2005;17;2378-85.
[28] Altosaar M, Raudoja J, Timmo K, Danilson M, Grossberg M, Krustok J, et al. Phys Status Solidi A 2008;205;167-70.
[29] Ganchev M, Iljina J, Kaupmees L, Raadik T, Volobujeva O, Mere A, et al. Thin Solid Films 2011;519;7394-8.

Table 1: Effect of residence time on composition and crystallite size.

Residence time, min	Composition, atomic %				Crystallite size, nm
	Cu	Zn	Sn	S	
< 1	44.15	1.36	15.37	39.13	7.6
28	33.19	0.88	14.52	51.44	8.6
49	33.77	6.27	12.12	47.85	13.8

Figure 1: (a) XRD and (b) Raman spectra for CZTS nanoparticles synthesized using stoichiometric precursors for different residence times. The composition, as determined by EDS, is also shown.

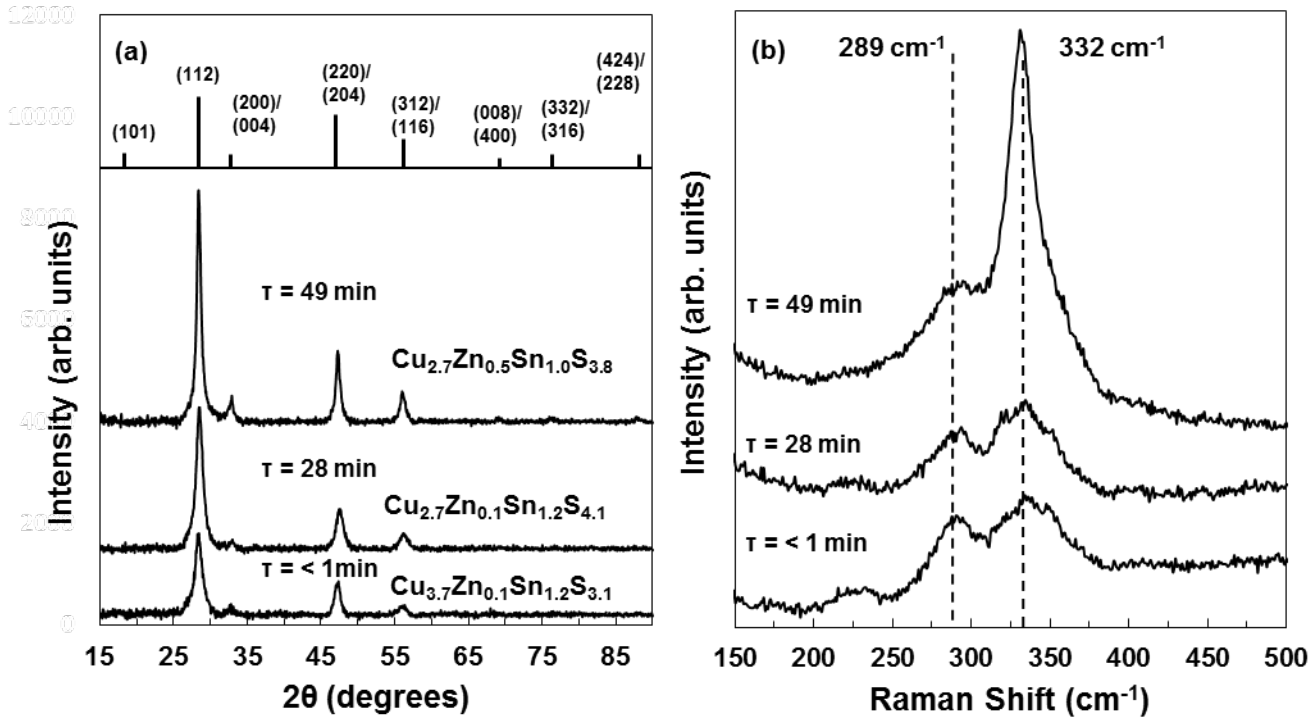

Figure 2 – TEM results for CZTS nanoparticles synthesized using optimized precursors shows that the CZTS nanoparticles were both (a,c) multicrystalline and (b,d) single crystalline with an (e) average size of 5.4 nm.

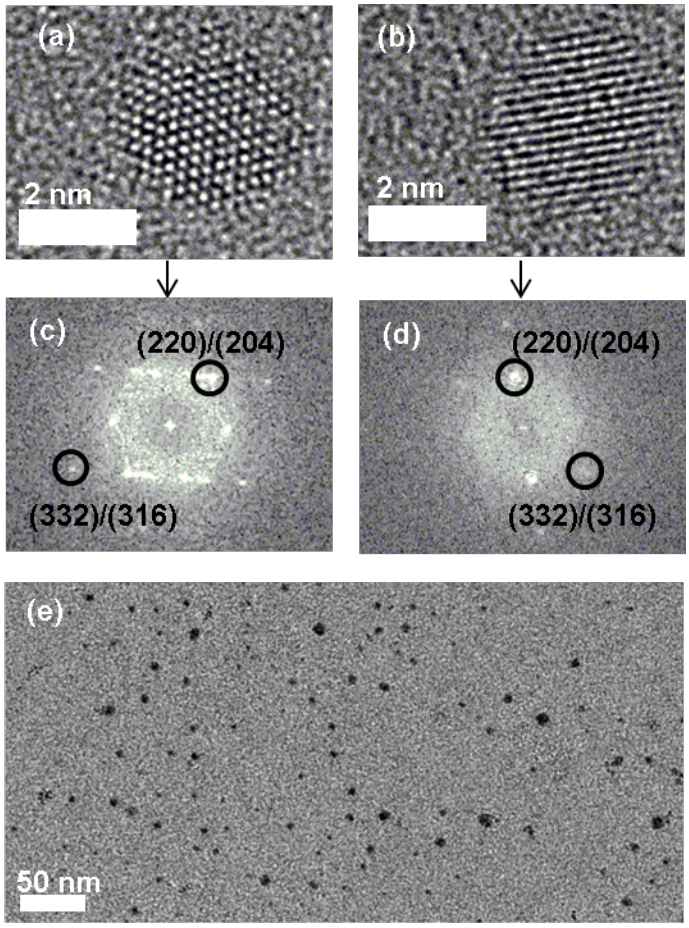

Figure 3: (a) XRD and (b) Raman for CZTS nanoparticles synthesized using optimized precursors and after annealing in N_2, N_2+S, and N_2+Se.